PNG1, a Yeast Gene Encoding a Highly Conserved Peptide:*N*-glycanase

Tadashi Suzuki, Hangil Park, Nancy M. Hollingsworth, Rolf Sternglanz, and William J. Lennarz

Department of Biochemistry and Cell Biology, Institute of Cell and Developmental Biology, State University of New York at Stony Brook, Stony Brook, New York 11794-5215

Abstract. It has been proposed that cytoplasmic peptide:*N*-glycanase (PNGase) may be involved in the proteasome-dependent quality control machinery used to degrade newly synthesized glycoproteins that do not correctly fold in the ER. However, a lack of information about the structure of the enzyme has limited our ability to obtain insight into its precise biological function. A PNGase-defective mutant (*png1-1*) was identified by screening a collection of mutagenized strains for the absence of PNGase activity in cell extracts. The *PNG1* gene was mapped to the left arm of chromosome XVI by genetic approaches and its open reading frame was identified. *PNG1* encodes a soluble protein that, when expressed in *Escherichia coli*, exhibited PNGase activity. *PNG1* may be required for efficient proteasome-mediated degradation of a misfolded glycoprotein. Subcellular localization studies indicate that Png1p is present in the nucleus as well as the cytosol. Sequencing of expressed sequence tag clones revealed that Png1p is highly conserved in a wide variety of eukaryotes including mammals, suggesting that the enzyme has an important function.

Key words: proteasome • de-*N*-glycosylation • quality control

Introduction

Proteins that transit through the secretory pathway are subjected to an ER quality control surveillance system that distinguishes aberrant proteins from folded proteins so that the former can be retained in the ER (Hammond and Helenius, 1995). In some cases, it has been shown that these misfolded and/or unfolded proteins are degraded by a so-called ER-associated degradation mechanism, which involves the ubiquitin-proteasome system (Kopito, 1997; Cresswell and Hughes, 1997; Suzuki et al., 1998a; Brodsky and McCracken, 1999; Plemper and Wolf, 1999; Römisch, 1999). Characterization of this process is important because the misfolding and degradation of certain glycoproteins causes a number of human genetic disorders.

In mammalian cells, there are examples when de-*N*-glycosylated intermediates in the overall degradation process can be detected in the presence of proteasome inhibitors (Wiertz et al., 1996a,b; Halaban et al., 1997; Hughes et al., 1997; Huppa and Ploegh, 1997; Yu et al., 1997; Bebök et al., 1998; de Virgilio et al., 1998; Johnston et al., 1998; Mosse et al., 1998; Yang et al., 1998). This de-*N*-glycosylation process is catalyzed by the action of a soluble peptide:*N*-glycanase (EC3.5.1.52; PNGase),[1] which is known to occur in mammalian cells (Suzuki et al., 1993; Kitajima et al., 1995), hen oviduct (Suzuki et al., 1997), as well as in the budding yeast, *Saccharomyces cerevisiae* (Suzuki et al., 1998b). PNGase cleaves the amide bond between the proximal *N*-acetylglucosamine and the linker asparagine residues on glycopeptides/glycoproteins, releasing an intact oligosaccharide and generating at the site of cleavage an aspartic acid residue in the peptide/protein backbone. PNGase has been widely used as a tool in studies on N-linked glycan chains. It has been shown that soluble PNGases have in common a neutral pH optimum for activity and a requirement for –SH groups (Suzuki et al., 1994a, 1997, 1998b; Kitajima et al., 1995). Genes encoding distinct classes of PNGases have been identified in *Chryseobacterium meningosepticum* and *Aspergillus niger* (Tarentino et al., 1990; Ftouhi-Paquin et al., 1997). These PNGases have no structural homology with each other; they are secreted and differ from the ubiquitous intracellular (cytoplasmic) PNGases in terms of enzymatic properties. Until now, the genes encoding the soluble PNGases involved in proteasomal degradation of proteins in eukaryotes have not been identified.

Address correspondence to William J. Lennarz, Department of Biochemistry and Cell Biology, Institute of Cell and Developmental Biology, State University of New York at Stony Brook, Stony Brook, NY 11794-5215. Tel.: (631) 632-8560. Fax: (631) 632-8575. E-mail: wlennarz@notes.cc.sunysb.edu

[1]*Abbreviations used in this paper*: CPY, carboxypeptidase; EST, expressed sequence tag; FOA, 5-fluoroorotic acid; GFP, green fluorescent protein; ORF, open reading frame; PNGase, peptide:*N*-glycanase

This study describes the PNGase gene (*PNG1*) from *S. cerevisiae*. A PNGase-defective mutant (*png1-1*) was identified by screening a collection of temperature-sensitive mutants for the loss of PNGase activity in cell extracts. The *PNG1* gene was mapped to the left arm of chromosome XVI by genetic approaches. The open reading frame (ORF) encoding Png1p was determined by performing PNGase activity assays on extracts derived from individual yeast strains that had a deletion of a particular ORF in a known position on chromosome XVI. In this way, one strain was found that was null in enzyme activity because it lacked the *PNG1* gene. *PNG1* was found to encode a 42.5-kD soluble protein with no apparent signal sequence. The *PNG1* gene was demonstrated to encode PNGase by expression of the enzymatically active protein in *E. coli*. Although *PNG1* is not an essential gene, it was found to be required for efficient degradation of a carboxypeptidase Y mutant protein that does not undergo folding. Subcellular localization studies indicate that the Png1p is found in the nucleus, with a lower level occurring in the cytoplasm. Comparison of the protein sequences with a variety of databases, followed by sequencing of a variety of expressed sequence tag (EST) clones, revealed highly related genes in humans, mice, plants, fruit flies, nematodes, and fungi, indicating that this class of PNGase is a highly conserved enzyme in eukaryotic cells.

Materials and Methods

Yeast Strains and Media

The yeast strains used in this study are listed in Table I. For screening of the collection of temperature-sensitive strains, 440 previously isolated mutant strains (Hartwell, 1967) were assayed. Unless otherwise noted, 10 ml of cells were grown at 30°C (or 25°C for temperature-sensitive strains) in YPAD (1% bacto-yeast extract, 2% bacto-peptone [both from Difco], 2% dextrose [J.T. Baker], and 40 mg/l adenine sulfate [Sigma Chemical Co.]) in a 50-ml centrifuge tube with shaking. Unless noted, standard yeast media and genetic techniques were used (Rose et al., 1990; Sherman, 1991; Elble, 1992).

PNGase Activity Assay

PNGase activity was assayed in yeast lysates using fetuin-derived asialoglycopeptide I ($[^{14}C]CH_3)_2$Leu-Asn($GlcNAc_5Man_3Gal_3$)-Asp-Ser-Arg) as described previously (Suzuki et al., 1994a, 1998b). Radioactivity was monitored on a PhosphorImager (Molecular Dynamics) and quantitated using ImageQuant (version 1.2). One unit was defined as the amount of enzyme that catalyzes hydrolysis of 1 μmol of fetuin-derived asialoglycopeptide I per minute.

Table I. Yeast Strains Used in this Study

Strain	Genotypes	Sources
W303-1a	MATa *ade2-101 his3-11,15 leu2-3,112 trp1-1 ura3-1 can1-100*	Laboratory stock
W303-1b	MATα *ade2-101 his3-11,15 leu2-3,112 trp1-1 ura3-1 can1-100*	Laboratory stock
PS593	MATα *ade2-1 leu2-3,112 trp1-289 ura3-52*	P. Sorger
K396-22B	MATα *ade1 his1 leu2 lys7 met3 trp5 ura3 spo11*	R. Esposito
K393-35C	MATα *his2 leu1 lys1 met4 pet8 ura3 spo11*	R. Esposito
K382-19D	MATα *ade2 his7 hom3 tyr1 ura3 can1 cyh2 spo11*	R. Esposito
K381-9D	MATα *ade6 arg4 aro7 asp5 lys2 met14 pet17 trp1 ura3 spo11*	R. Esposito
BY4742	MATα *his3Δ1 leu2Δ0 lys2Δ0 ura3Δ0*	This study
#2156	MATα *his3Δ1 leu2Δ0 met15Δ0 ura3Δ0 png1Δ::KanMX4*	Research Genetics
#10568	BY4742 *erg6Δ::KanMX4*	Research Genetics
#20941	MATa/MATα *his3Δ1/his3Δ1 leu2Δ0/leu2Δ0 lys2Δ0/LYS2 met15Δ0/MET15 ura3Δ0/ura3Δ0 spo11Δ::KanMX4/SPO11*	Research Genetics
RSY281	MATα *sec23-1 ura3-52 his4-619*	R. Schekman
RSY607	MATα *leu2,3-112 ura3-52 pep4Δ::URA3*	R. Schekman
CY629	MATα *his3-Δ200 leu2-Δ1 trp1-Δ63 ade-2-101 lys2 hho1Δ::HIS3*	C. Peterson
YEA78	W303-1b *hmr::URA3 Δeb::UAS_G gal4Δ::LEU2*	R. Sternglanz
YWC2	W303-1a *elp3Δ::URA3*	R. Sternglanz
TSY5	MATa *ade2 his3 leu2 trp1 ura3 png1-1*	This study
TSY9	MATα *ade2 his3 leu2 trp1 ura3 png1-1 can1*	This study
TSY41	TSY5 *spo11Δ::ADE2*	This study
TSY54	TSY41 *can1 cyh2*	This study
TSY75*	MATα *ade6 aro7 lys2 met14 trp1 ura3 sec23-1 (spo11)*	This study
TSY79	MATα *ade2 his3 leu2 trp1 ura3 gal4Δ::LEU2*	This study
TSY80	MATa *ade2 his3 leu2 trp1 ura3 gal4Δ::LEU2*	This study
TSY82	MAT*a ade2 his3 leu2 trp1 ura3 gal4Δ::LEU2 hho1Δ::HIS3*	This study
TSY83	MATα *his3Δ1 leu2Δ0 lys2Δ0 met15Δ0 ura3Δ0 spo11Δ::KanMX4*	This study
TSY91	MATα *ade2 his3 leu2 trp1 ura3 can1 gal4Δ::LEU2 elp3Δ::URA3*	This study
TSY94	MATα *ade2 his3 leu2 ura3 gal4Δ::LEU2 pep4Δ::URA3*	This study
TSY115	#2156 *prc1-1*	This study
TSY146	W303-1a *png1Δ::$his5^+$(pombe)*	This study
TSY147	BY4742 *prc1-1*	This study
TSY148	BY4742 *prc1-1 erg6Δ::KanMX4*	This study
TSY149	BY4742 *prc1-1 png1Δ::KanMX4*	This study
TSY150	BY4742 *prc1-1 erg6Δ::KanMX4 png1Δ::KanMX4*	This study

*Parentheses indicate phenotype was not determined.

Chromosomal Identification of png1-1 Locus

To generate TSY41, SPO11 gene disruption of TSY9 was carried out using SalI-PvuII digests of pME302 (Engebrecht and Roeder, 1989). The disruption was confirmed by showing that when crossed to a spo11 tester strain and sporulated, <1% of the spores were viable. Furthermore, spore inviability was complemented by the introduction of pGB430 (provided by Dr. J. Engebrecht, SUNY at Stony Brook) containing the wild-type SPO11 gene. Chromosomal mapping of png1-1 mutation was performed using the spo11-mapping method (Klapholz and Esposito, 1982). For mapping of chromosome XII, TSY83 was prepared by sporulation of Research Genetics strain (No. 20941). Can^R and Cyh^R derivatives of TSY41 cells (TSY54) were isolated by selecting cells on plates containing either synthetic media –Arg +60 μg/ml canavanine or YPAD +10 μg/ml cycloheximide. The mutants were shown to be mutant for CAN1 and CYH2 by complementation tests.

Genetic Mapping of png1-1 Locus

TSY75, which carries *aro7* and *sec23* as markers for the right arm of chromosome XVI, was prepared by crossing RSY281 (a gift from Dr. Randy Schekman, University of California at Berkeley, Berkeley, CA) with K398-4D and isolating haploid segregants of the appropriate genotype. TSY82, which carries *hho1Δ::HIS3* and *gal4Δ::LEU2* as markers on the left arm of chromosome XVI, was prepared by crossing CY629 with YEA78 and isolating haploid segregants of the appropriate genotype. These strains were crossed to *png1-1* haploids (TSY5 or TSY9, respectively), and tetrad analysis of the resulting spores determined whether *png1-1* was linked to any of the markers.

To carry out mitotic mapping to determine the proximity of the mutation to known markers, TSY94 (prepared by crossing RSY607; a gift from Dr. Randy Schekman) with TSY80 and isolating haploid segregants of the appropriate genotype and TSY91 (prepared by crossing TSY79 with YWC2 and isolating haploid segregants of the appropriate genotype) were used. After mating these strains with TSY9, diploids were selected. The diploids were grown nonselectively overnight at 30°C in YPAD and plated to select for FOA^R colonies. Among these, Leu^- cells were assayed for PNGase activity.

Bacterial Expression of Png1p

DNA manipulations were performed according to Sambrook et al. (1989). The full-length PNG1 sequence was amplified from yeast chromosomal DNA using Vent DNA polymerase (New England BioLabs, Inc.) using 5′ primer (5′-TTTTTCCATGGGAGAGGTATACGAAAAAA-3′) and 3′ primer (5′-TTTTTCTCGAGCTATTTACCATCCTCCCCAC-3′). Thus, the fragment obtained was cut by NcoI-XhoI digestion, and cloned into NcoI-SalI–digested pET-28b (Novagen, Inc.). For the $(His)_6$ version of Png1p, another 3′ primer (5′-TTTTTCTCGAGTTTACCATCCTCCCCACGCT-3′) was used, and the NcoI-XhoI fragment was cloned into the pET-28b vector. These constructs were transformed into BL21(DE3) pLysS cells, and expression of PNG1 was induced by adding 1 mM IPTG at OD_{600} = 0.8/ml. After 3 h at 37°C, 3 ml of cells were collected and the protein was extracted by adding 400 μl of PBS/1% Triton containing 5 mM DTT and 1 mM PMSF, followed by sonication on ice using a Branson sonicator at level 3 for two 10-s intervals with a 1-min wait at 0°C between sonications. The cell extract was centrifuged at 16,000 *g* for 10 min at 4°C, and the supernatant was assayed for PNGase activity.

Purification of $(His)_6$-tagged Png1p (Png1$(His)_6$p)

The overproduced $(His)_6$-tagged Png1p (Png1$(His)_6$p) in *E. coli* as described above was purified using a TALON metal affinity resin (CLONTECH Laboratories, Inc.). The *E. coli* extract (15 ml) was obtained as described above, except that the extract was made in 20 mM Tris-HCl buffer/1% Triton, pH 7.5, and 1 mM PMSF. Thus, the extract obtained was incubated at 4°C for 2 h with 0.5 ml Talon resin that had been preequilibrated with 20 mM Tris-HCl/100 mM NaCl (binding buffer, pH 7.5). The entire reaction was transferred into a 3-ml gravity flow column, and the flowthrough fraction (~3 ml) was collected. The resin was further washed with binding buffer with 10 mM imidazole (4 ml), and then eluted with binding buffer with 100 mM imidazole (4 ml). Finally, the column was washed with 40 mM MES-NaOH buffer, pH 5.2. Throughout the column operation, fractions of 1 ml were collected. During fractionation, DTT was immediately added to each fraction to a final concentration of 10 mM. Each fraction was analyzed by SDS-PAGE and also was assayed for PNGase activity. The pure Png1$(His)_6$p fraction (fraction 8–12) was collected, concentrated with B88 buffer (20 mM Hepes-KOH buffer, pH 6.8, 150 mM potassium acetate, 5 mM magnesium acetate, and 250 mM sorbitol) containing 10 mM DTT using a Microcon 10 (Amicon Inc.), and finally diluted with B88 with 10 mM DTT at a final concentration of 14 μg protein/ml. The protein concentration was quantitated with the Bio-Rad protein assay kit.

Product Analysis of Incubation of [^{14}C]Asialofetuin Glycopeptide I with Purified Png1$(His)_6$p

Deglycosylation reaction by purified Png1$(His)_6$p was confirmed by product analysis using paper chromatography and paper electrophoresis as described earlier (Kitajima et al., 1995). [^{14}C]Asialofetuin glycopeptide I (20,000 dpm) was digested with 12 μU of purified Png1$(His)_6$p, in a 10-μl reaction with 40 mM MES-NaOH buffer, pH 6.6, with 10 mM DTT at 30°C for 15 h. The paper chromatography steps detect the removal of the glycan from glycopeptide, whereas the paper electrophoresis confirms the conversion of a glycosylated asparagine residue into an aspartic acid residue (Kitajima et al., 1995). Paper chromatography was carried out using 1-butanol/ethanol/H_2O = 2:1:1 as a solvent (Suzuki et al., 1998b). Paper electrophoresis was carried out using a model EF-200 unit (Advantec Toyo Kaisha Ltd.) as described earlier (Suzuki and Lennarz, 2000) and visualized using a PhosphorImager. Authentic PNGase F-deglycosylated peptide was prepared by digestion of 20,000 dpm [^{14}C]asialofetuin glycopeptide I with 5 units of PNGase F (Roche) in 20 μl of 50 mM Tris-HCl buffer, pH 8.0, at 37°C for 15 h.

Examination of Reactivity of Purified Png1$(His)_6$p toward Glycoproteins In Vitro

10 μg each of three glycoproteins, ovalbumin, ribonuclease B, and carboxypeptidase Y (Sigma Chemical Co.) was incubated in 20 μl of 40 mM MES-NaOH buffer, pH 6.6, containing 10 mM DTT with 30 μU of purified Png1$(His)_6$p at 30°C for 15 h. For reference, 10 μg of each glycoprotein was digested with 2 μl of PNGase F (a gift from Dr. Robert Haltiwanger, SUNY at Stony Brook) in 20 μl of 50 mM Tris-HCl buffer, pH 8.5, at 37°C for 15 h. The reaction mixture was analyzed by 8% (carboxypeptidase Y), 10% (ovalbumin) or 15% (ribonuclease B) SDS-PAGE. In one experiment, glycoproteins were preincubated at 65°C for 30 min at a concentration of 1 mg/ml before incubation with Png1$(His)_6$p.

Construction of PNG1-containing Plasmids for Expression in Yeast

The *PNG1* allele including its promoter region was amplified from yeast genomic DNA using the following primers and Vent DNA polymerase: 5′-AAAAAGAATTCCGTACAAACAAGCTAGAG; and 5′-AAAAACTCGAGTCACACCAGGCTATGAGGG-3′. The fragment obtained was digested with EcoRI-XhoI, and was cloned into the EcoRI-XhoI site of pRS316 (Sikorski and Hieter, 1989), or the EcoRI-SalI site of YEp352 (Hill et al., 1993). These plasmids were transformed into a *PNG1* deletion strain (TSY146), and the protein extract was prepared from cells (total OD_{600} = 40) by the method described earlier (Suzuki et al., 1998b). The PNGase activity in each extract was assayed as described above.

For analyzing the mutation in *png1-1*, genomic DNA was isolated from TSY5, and the *png1-1* allele was isolated by PCR using the same primers as described above. The fragment obtained was digested with EcoRI-XhoI, and was cloned into the EcoRI-XhoI site of pBluescript II S/K (+/−) (Strategene) for sequencing and the EcoRI-SalI site of YEp352 for expression of this allele in TSY146 cells.

Construction of Carboxypeptidase Mutant (CPY)*

The *prc1-1* mutation was introduced into yeast using the two-step gene replacement method (Rothstein, 1991). An integrating plasmid containing *prc1-1* was constructed using the PCR mutagenesis technique (Horton et al., 1990). In brief, the EcoRI-HindIII fragment of pJW1433, which contains the ORF of wild-type *PRC1* (Holst et al., 1996), was cloned into YIp5 (New England Biolab). pJW1433 was a gift from Dr. Jacob Winther (Carlsberg Laboratory, Copenhagen Valby, Denmark). The following primers were used to amplify a fragment of *PRC1* using pJW1433 as a template: 5′-GGTTACTTGGATGTGGAAGACG-3′; 5′-CCACATCGCTAGGGAATCCTAC-3′; 5′GTAGGATTCCCTAGCGATGTGG-3′; and 5′-CAAAAGATCTGTTACGGCGGTG-3′ (underlined letters re-

fer to base change used to generate CPY*). The fragment was digested with AocI-BglII, and the equivalent fragment on YIp5-CPY was replaced by the PCR-derived *prc1-1* fragment. The sequence was confirmed using the EXCELII sequencing kit (Epicentre Technologies). The YIp5-CPY* was cut by AocI and integrated into strains of *PRC1* locus. Transformants were grown nonselectively in YPAD to allow excision of the plasmid and plated onto FOA plates. The presence of *prc1-1* was confirmed by showing disruption of the BstXI site within the gene using colony PCR as described before (Jakob et al., 1998). For PCR, the following primers were used: 5′-TTGAAACCCATCGGGAACCC-3′ and 5′-ACAACGTTCCAAAGGGTCTTC-3′; and the digests were analyzed in a 2% agarose gel.

Radiolabeling of Cells and Immunoprecipitation

Cells were grown to an OD_{600} = 1 at 30°C in minimal medium without methionine and cysteine. Cells were concentrated to OD_{600} = 10, and 1-ml aliquots were preincubated at 30°C for 30 min. During the preincubation, where indicated, MG-132 (Calbiochem) was added to a final concentration of 50 μM from a freshly made 5 mM solution in (DMSO). For control cells, the same amount of DMSO was added. Radiolabeling of the cells was initiated by the addition of Easy Tag Express-[^{35}S] (43.48 GBq/mmol; NEN Life Science Products) to 100 μCi/OD_{600} of cells, and incubation was continued for 10 min for the *prc1-1* strain and 5 min for the *PRC1* strain. A chase mix was added from a 100× stock solution (0.3% cysteine and 0.4% methionine), and incubation continued. At indicated periods of time, an equal volume of ice-cold 20 mM NaN_3/20 mM Tris-HCl, pH 7.5, was added to terminate the chase. Protein extracts were prepared and were immunoprecipitated as described previously (Gillece et al., 1999) using anti-CPY antiserum (a gift from Dr. Marcus Aebi, ETH, Zürich). Proteins were analyzed on 7.5% polyacrylamide gels. When necessary, immunoprecipitated samples were divided into two aliquots; one was treated with 5 U of PNGase F (Roche) for 16 h at 37°C before gel electrophoresis. Labeled bands were visualized using the PhosphorImager and quantitated as described above. The cells used for this analysis (TSY147-150) were made by crossing TSY115 with Research Genetics strain No. 10568 and isolating haploid segregants of the appropriate genotype.

Western Blot Analysis

Protein extracts (20 μg) from yeast cells were prepared as described (Yan et al., 1999). Extracts were resolved on 10% SDS-PAGE and transferred to nitrocellulose membranes. Blots were incubated with a 1:100 dilution of anti-GFP mAb (CLONTECH Laboratories, Inc.), followed by 1:2,000 dilution with the anti-mouse IgG HRP-conjugated secondary antibody (Roche). Gels were visualized using chemiluminescence (Kpn) after exposure to medical X-ray film (Fuji Photo Film Co.).

Construction of Png1-GFP Fusion Protein and Determination of Subcellular Localization of Png1p

A *png1*Δ strain in a W303-1a background was made by the one-step PCR-mediated technique for deletion using the *Schizosaccharomyces pombe his5*$^+$ gene (Longtine et al., 1998). The pFA6a-His3MX6 was used as a template and the following primers were used for amplifying the disruption cassette: 5′-AGATATAGAAGACGTAAAACAACCTGAAGAAGGTAACAGGTGGAGTAGCACGGATCCCCGGGTTAATTAA-3′; and 5′-CTGGTTAACAAAGCAAGCTGCCGAGTTCTTGGGCAGC-TTTGATGAGTTAGGAATTCGGGCTCGTTTAAAC-3′. The disruption was verified by PCR as well as by the loss of PNGase activity in the cell extract.

A plasmid encoding a green fluorescent protein (GFP) fusion at the COOH terminus of Png1p was made using pGFP-C-FUS plasmid (Niedenthal et al., 1996), in which the protein can be expressed under the control of the *MET25* promoter. In brief, the XbaI-HindIII fragment from $(His)_6$-tagged *PNG1* in pET-28b was cloned into equivalent sites of the pGFP-C-FUS plasmid. The fusion protein was expressed in the synthetic medium -Ura-Met, and 5 ml of logarithmically growing cells (OD_{600} = 0.6/ml) were fixed for 3 h in the growth medium supplemented with 3.7% formaldehyde and 40 mM potassium phosphate buffer, pH 6.5, containing 0.5 mM $MgCl_2$. Cells were washed once and resuspended in 0.5 ml of sorbitol buffer (1.2 M sorbitol, 40 mM potassium phosphate buffer, pH 6.5, and 0.5 mM $MgCl_2$). Cell walls were digested for 30 min at room temperature in sorbitol buffer supplemented with 0.2% β-mercaptoethanol and 30 μl of 10 mg/ml zymolyase-100T (ICN). The resulting spheroplasts were placed on poly-L-lysine–coated glass slides and mounting media (50 ng/ml DAPI and 1% p-phenylenediamine in PBS, pH 8.0). Images of GFP fluorescence as well as DAPI staining were captured in Adobe Photoshop from a SPOT-cooled CCD 24-bit color digital camera (Diagnostic Instruments) mounted on a Zeiss Axioskop 2 microscope using the software supplied with the SPOT camera.

Determination of PNG1-related Gene Sequences

Sequence similarity searches were performed on the National Center of Biotechnology Information (NCBI) server (http://www.ncbi.nlm.nih.gov), the Berkeley Drosophila Genome Project (BDGP) server (http://www.fruitfly.org), and the *C. elegans* EST database of the DNA Databank of Japan (DDBJ; http://www.ddbj.nig.ac.jp/htmls/c-elegans/html/CE_INDEX.html). Mouse EST clones were first identified (see Table IV) based on their sequence similarity to the yeast Png1p sequence. One of these EST clones (AI019191) was sequenced, and the sequences obtained were used to find other clones. cDNA clones (ID No. 948982, 1316890 and LD46390) were obtained from Research Genetics; EST (ID 97076) was obtained from American Type Culture Collection, and the *C. elegans* EST clone (yk491h3) was a gift from Dr. Yuji Kohara (National Institute of Genetics). All EST clones were completely sequenced, and deduced amino acid sequences were obtained using MacVector (version 6.0). Detailed methods can be provided upon request.

Results

Isolation of a PNGase-defective Mutant from a Temperature-sensitive Mutant Collection

Earlier we reported that *S. cerevisiae* has a soluble PNGase activity that is very similar in terms of enzymatic properties to the soluble PNGases found in higher eukaryotes (Suzuki et al., 1998b). To identify the PNGase gene in yeast, mutants defective in PNGase activity were sought. From a collection of temperature-sensitive mutants, 440 strains were individually assayed for the loss of PNGase activity (Hartwell, 1967). Among these 440 strains, 10 strains showed virtually no PNGase activity at 37°C, the nonpermissive temperature. These 10 strains were crossed to an isogenic strain (PS593). The resulting diploids were dissected and individual spore colonies were assayed for PNGase activity. One strain (No. 352) was observed to segregate 2^+:2^- for PNGase activity in this cross (Fig. 1), demonstrating that the PNGase defect in strain No. 352 was the result of a mutation in a single gene. The PNGase defect in No. 352 did not cosegregate with the temperature-sensitive phenotype (data not shown). We named the mutation in the strain *png1-1*, after peptide:*N*-glycanase. Strains TSY5 and TSY9 (see Table I for a complete strain list) carrying *png1-1* were made by backcrossing strain No. 352 with wild-type strains (one cross with PS593 followed by four crosses with W303-1 strain), and used for the mapping study.

Chromosomal Mapping of png1-1 Mutation

Neither TSY5 nor TSY9 showed any phenotype or growth defect under various experimental conditions tested, making it difficult to clone by complementation. Therefore, the *spo11* mapping technique (Klapholz and Esposito, 1982) was employed to localize the *png1-1* mutation onto a particular chromosome. The rationale behind this approach takes advantage of the fact that there is no meiotic recombination in *spo11* diploids. Therefore, if a *png1 spo11* haploid is crossed to a *spo11* strain carrying *lys1* on chromosome IX, for example (thereby producing a diploid with the parental configuration (*png1 LYS1*/*PNG1 lys1*)),

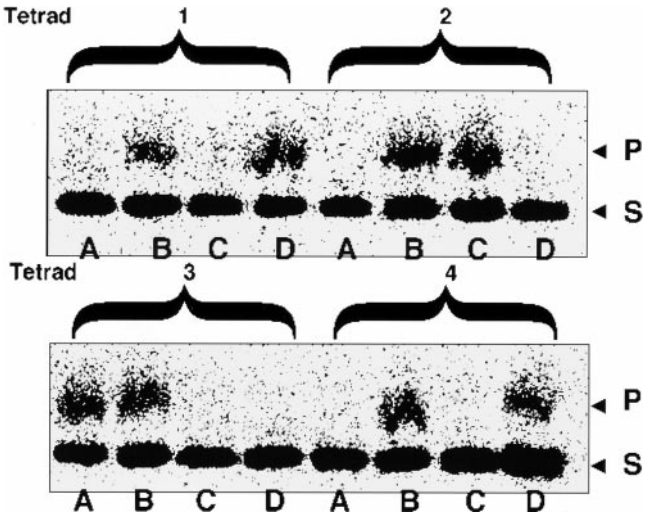

Figure 1. Assay of PNGase activity in four sets of tetrads from the cross of a PNGase-defective mutant (No. 352) with a wild-type strain (PS593). Protein extracts (~20 μg) from each spore colony were incubated with 25 μM of [^{14}C]asialofetuin peptide I in 6 μl of 70 mM Hepes-NaOH buffer, pH 7.2, and 5 mM DTT at 25°C for 16 h. The reaction product was analyzed by paper chromatography and the radioactive peptides were visualized using a PhosphorImager. A paper chromatogram of four different tetrads (1–4) are shown. P, de-*N*-glycosylated product ([^{14}C]-Leu-*Asp*-Asn-Ser-Arg); and S, substrate ([^{14}C]-Leu-Asn($GlcNAc_5Man_3Gal_3$)-Asn-Ser-Arg).

recombinant spores (*PNG1 LYS1* and *png1 lys1*) arise primarily by independent assortment during meiosis. The presence of recombinant spores is, therefore, suggestive that *png1* is not on the marked chromosome. In contrast, the absence of recombinant types suggests that *png1* is located on the same chromosome as that marker. Because *spo11* mutants produce predominantly inviable spores, rare viable spores were first selected on –Arg plates containing canavanine and cycloheximide (Hollingsworth and Byers, 1989). The spore colonies were patched onto YPAD plates and replica plated onto the appropriate media to score the marked chromosomes. PNGase assays were performed on the spore colonies to determine the *png1* phenotype.

The data in Table II show that the cross between *aro7* and *png1-1* was the only one to produce a class of no recombinant types (*png1 aro7*). The other seven putative recombinants (Tyr^+ $PNGase^+$) were demonstrated by further genetic analysis to be due to disomy of chromosome XVI resulting from nondisjunction (data not shown). Therefore, these results suggested that *png1-1* was on chromosome XVI.

Genetic Mapping of png1-1 Mutation to a Specific Site on Chromosome XVI

To localize *png1-1* more precisely on chromosome XVI, *png1-1* was crossed to TSY75 and TSY82, both of which have two markers (*ARO7* and *SEC23* in TSY75 and *HHO1* and *GAL4* in TSY82) on chromosome XVI (Fig. 2). Tetrad analysis of the sporulated diploids revealed that the

*Table II. Segregation of png1-1 Mutation with Other Markers on spo11 Mapping Analysis**

Chromosome (marker‡)	Phenotype of spores			
	Parental 1	Parental 2	Recombinant 1	Recombinant 2
I (*ade2*)	7	7	5	10
II (*lys2*)	14	8	5	4
III (*leu2**)	21	23	12	13
IV (*trp1**)	11	20	9	11
V (*hom3*)	NA‖	22	NA‖	12
VI (*his2*)	6	7	2	7
VII (*cyh2*)	2	14	8	11
VIII (*arg4*§)	11	6	7	7
IX (*lys1*)	3	3	5	10
X (*met3*)	4	3	4	3
XI (*met14*)	16	4	9	2
XII (*met15*)	2	1	2	3
XIII (*lys7*)	9	9	11	6
XIV (*met4*)	1	4	7	10
XV (*his3**)	26	13	31	14
XVI (*aro7*)	23	34	7	0

*The results shown were obtained by cross of TSY54 to test strains (K396-22B/K381-9D/K393-35C/TSY83) except for chromosome V (*hom3*) and chromosome VII (*cyh2*), which were obtained from TSY41 × K382-19D, selecting spores only using canavanine.
‡The markers indicated with asterisks were from TSY54, whereas the others were from the test strains.
§Spores were selected using only cycloheximide.
‖NA, not applicable because of the selection method.

png1-1 mutant was not linked to markers on the right arm, whereas *png1-1* did exhibit linkage to the HHO1 locus, but not to *GAL4*, on the left arm (Table III). These results placed the *png1-1* mutation approximately in the middle region of the left arm on chromosome XVI.

To further narrow down the *png1-1* locus, mitotic mapping was carried out. This method uses mitotic crossing over in diploids to determine the order of genes on the same arm of a chromosome. TSY91 contains *URA3* integrated at the *ELP3* locus and TSY94 contains *URA3* integrated at the *PEP4* locus. These strains were crossed to the *png1-1 ura3* haploid TSY5. The diploids were grown nonselectively and plated on 5-fluoroorotic acid (FOA) to select for strains exhibiting loss of the *URA3* gene. This loss of heterozygosity results from crossovers between either *elp3*Δ*::URA3* or *pep4*Δ*::URA3* and centromere. To ensure that FOA^R was due to recombination and not gene conversion, loss of the *gal4*Δ*::LEU2* marker on the same arm distal to *elp3*Δ*::URA3* and *pep4*Δ*::URA3* was also re-

Table III. Genetic Mapping of the png1-1 Mutation by Tetrad Analysis

Cross	Parental Ditypes	Nonparental Ditypes	Tetratypes	Linkage
png1-1 × SEC23*	3	4	8	unlinked
png1-1 × ARO7*	3	4	8	unlinked
png1-1 × HHO1‡	15	0	6	14.3 cM
png1-1 × GAL4‡	4	2	15	unlinked

*The results shown were obtained by crossing TSY5 with TSY75.
‡The results shown were obtained by crossing TSY9 with TSY82.

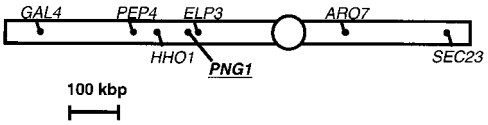

Figure 2. Schematic representation of chromosome XVI of *S. cerevisiae* and the marker genes used in this study. The *PNG1* locus determined in this study is also indicated.

quired. All of the FOA^R Leu$^-$ colonies derived from the TSY5/TSY91 diploid were defective for PNGase activity, indicating that the *png1-1* locus is distal to the *ELP3* locus. On the other hand, 4/16 FOA^R Leu$^-$ strains were PNGase-positive from the TSY5/TSY94 diploid, indicating that the *png1-1* gene is centromere proximal to the *PEP4* locus.

Given that *png1-1* is located in between *ELP3* and *PEP4*, the *Saccharomyces* Genome database (http://genome-www.stanford.edu/Saccharomyces/) was analyzed for ORFs in this interval. Among 67 ORFs, 16 candidate ORFs were chosen (*YPL144w*, *YPL141c*, *YPL138c*, *YPL136w*, *YPL116w*, *YPL113c*, *YPL110c*, *YPL108w*, *YPL107w*, *YPL103c*, *YPL101w*, *YPL100w*, *YPL099c*, *YPL098c*, *YPL096w*, and *YPL095c*). These ORFs were chosen as potential candidates for *PNG1* based on the following criteria: (1) the ORF was uncharacterized; (2) it was at least 20 kb distance from the *HHO1* locus (based on tetrad analysis data); and (3) it encoded a protein with a molecular mass >12 kD. Strains containing individual deletions of each ORF were obtained from Research Genetics and assayed biochemically for PNGase activity. A strain deleted in *YPL096w* (No. 2156) did not exhibit any PNGase activity, thereby identifying this ORF as *PNG1*. To confirm that *png1-1* is the same locus as *YPL096w*, we crossed the Research Genetics strain (No. 2156) with the *png1-1* haploid, TSY9. After tetrad dissection, 10 tetrads were assayed for PNGase activity; none of the spores exhibited PNGase activity, as expected if the two mutants are allelic. Indeed, the sequence analysis of *png1-1* allele revealed that the *png1-1* allele was due to a point mutation of residue 218, in which His was mutated to Tyr mutation. The catalytic inactivity of this mutant protein is consistent with the fact that this His residue is highly conserved in a variety of eukaryotic organisms (see below).

PNG1 is predicted to encode a protein (Png1p) with a molecular mass of 42.5 kD. The protein does not have either a predicted signal sequence or a membrane spanning domain. Png1p does not have any homologues in the *S. cerevisiae* genome nor does it exhibit any sequence similarity with known PNGases from a bacterium and a fungus (Tarentino et al., 1990; Ftouhi-Paquin et al., 1997). However, a number of related proteins in other eukaryotes, including mammalian cells, were identified (see below).

Bacterial Expression of PNG1 Shows that Png1p Is a Soluble Enzyme

Although mutation of the *PNG1* gene renders yeast cells devoid of PNGase activity, this result by itself does not distinguish whether *PNG1* encodes the PNGase enzyme or a regulatory gene required for PNGase activity. Since no PNGase activity in *E. coli* extracts was observed under our

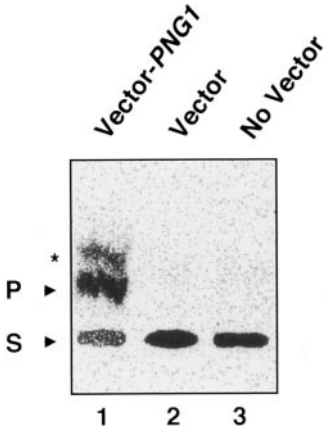

Figure 3. Assay of PNGase activity in an *E. coli* cell-free extract. The *E. coli* strain used was BL21(DE3)pLysS. Shown is a paper chromatogram of the reaction product formed after 10 min of incubation of the *E. coli* extract with labeled substrate. (lane 1) *E. coli* extract with pET-28b-*PNG1*; (lane 2) *E. coli* extract with pET-28b (control vector); and (lane 3) *E. coli* extract without vector. The extra minor band indicated with an asterisk was confirmed to be [^{14}C]Leu-*Asp* by analysis by paper electrophoresis, as described earlier (Kitajima, et al., 1995), and may be derived from a contaminating protease activity in the *E. coli* extract. In fact, this degradation product represents a fraction of the product of PNGase activity because the second amino acid in the substrate was converted into Asp instead of remaining as Asn. P, de-*N*-glycosylated product ([^{14}C]-Leu-*Asp*-Asn-Ser-Arg); and S, substrate ([^{14}C]-Leu-Asn(Glc $NAc_5Man_3Gal_3$)-Asn-Ser-Arg). For details, see Materials and Methods.

experimental conditions, the yeast *PNG1* gene was placed under the T7 expression system, introduced into *E. coli*, and the resulting cell extracts were monitored for PNGase activity. As shown in Fig. 3, expression of *PNG1* in BL21 (DE3)pLysS cells with the pET-28b vector resulted in very high PNGase activity. A similar result was observed in extracts from *E. coli* expressing (His_6)-tagged *PNG1* (data not shown). The protein was easily recovered from the soluble fractions after cell lysis with 1% Triton in the extraction buffer followed by centrifugation at 16,000 *g*.

For the purpose of subsequent product analysis using glycopeptide/glycoproteins as substrates, purification of Png1p was performed by using (His_6)tag and a (His_6)-tagged protein-specific metal affinity resin. In Fig. 4 (A and B), the elution profile of the *E. coli* extract overexpressing (His_6)-tagged Png1p (Png1(His_6)p) using a TALON metal affinity column is shown. The tightly bound fraction (Fractions 8–12) gave a single protein band ~44 K on SDS-PAGE (Fig. 4 A), which is consistent with the expected molecular mass of Png1(His_6)p. This bound protein, together with the flowthrough fraction, exhibited high PNGase activity (Fig. 4 B), which was quantitated by paper chromatography. The elution pattern of PNGase correlated with the appearance of the Png1(His_6)p band on the gel (Fig. 4, A and B). The purified protein exhibited 3 mU/ml of activity and the specific activity of pure protein was calculated to be 0.21 μmol of glycopeptide degraded/mg protein/min.

To rigorously prove that the reaction product detected by Png1p was formed by a de-*N*-glycosylation reaction, further product analysis was performed using the purified Png1(His_6)p. This was particularly important because the paper chromatographic method only detects the removal of the glycan from peptide, which could be catalyzed by another type of endoglycosidase such as endo-β-*N*-acetyl-

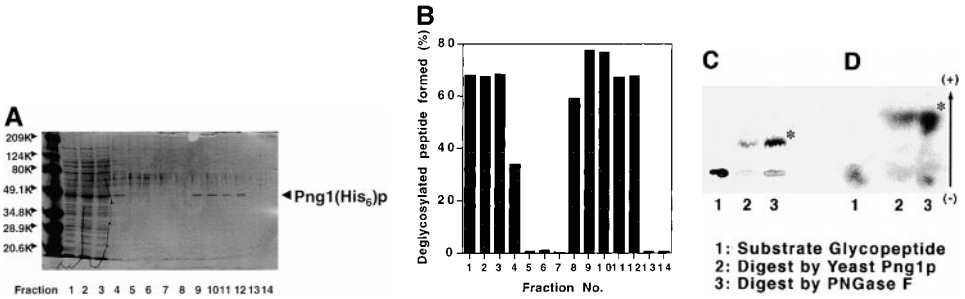

Figure 4. Purification of (His_6)-tagged Png1p (Png1(His_6)p) and reaction product analysis of [^{14}C]asialofetuin glycopeptide I with it. *E. coli* extract overexpressing Png1(His_6)p was incubated with TALON metal affinity resin, transferred to a 3-ml gravity flow column, and the elution was carried out as described in Materials and Methods. (A) Elution profile of each fraction was analyzed by 10% SDS-PAGE. 10 μl of each fraction was applied for the analysis. The position of migration of Png1(His_6)p is indicated. Molecular masses indicated are based on prestained molecular mass marker standards (Bio-Rad). (B) Detection of PNGase activity in each elution fraction. The activity in each fraction was measured after 16-h incubation of reaction mixture at room temperature. (C and D) Analysis of reaction products produced by incubation of [^{14}C]asialofetuin glycopeptide I with purified Png1(His_6)p using (C) paper chromatography and (D) paper electrophoresis. (lane 1) [^{14}C]asialofetuin glycopeptide I; (lane 2) reaction product formed by Png1(His_6)p; and (lane 3) reference reaction product formed by PNGase F. The PNGase-deglycosylated product, [^{14}C]-Leu-*Asp*-Asp-Ser-Arg, is indicated by asterisks.

glucosaminidase (Suzuki et al., 1995). For this purpose, paper electrophoresis analysis was performed since this method separates products primarily based on their charge and will detect the conversion of the glycosylated Asn into an Asp residue. This, together with the paper chromatography, has been established as the method to detect PNGase activity in cellular tissues (Kitajima et al., 1995). For a reference sample, PNGase F-deglycosylated peptide was used. Indeed, the reaction product from purified Png1(His_6)p gave the same mobility with the authentic deglycosylated peptide formed by PNGase F using paper electrophoresis as well as paper chromatography (Fig. 4, C and D). This clearly demonstrates that Png1p possesses PNGase activity.

To determine if there was a correlation of *PNG1* expression and PNGase activity, *PNG1* was expressed using CEN (pRS316; single copy) or 2-micron (YEp352; multicopy) plasmids in the *png1*Δ strain (TSY146). As shown in Fig. 5 A, both *PNG1* constructs complemented the defect of PNGase activity in *png1*Δ strain. A time course experiment (Fig. 5 B) showed that the PNGase activity was four- to fivefold higher in cells expressing Png1p with the 2-micron plasmid than that with CEN plasmid, indicating a clear-cut correlation of PNGase activity with the level of expression of *PNG1*.

To assess the reactivity of Png1p toward glycoproteins in vitro, three glycoproteins (ribonuclease B, ovalbumin, and carboxypeptidase Y) were examined. In sharp contrast to bacterial PNGase F, there was no detectable de-*N*-glycosylated product found by SDS-PAGE analysis, even after the proteins were heat treated to partially denature them (data not shown).

Deletion of PNG1 Causes a Delay in the Degradation of a Mutant Form of Carboxypeptidase Y

A phenotypic difference between wild-type and *png1*Δ cells was not detected in terms of growth rate or viability (data not shown). Because soluble PNGase activity has been proposed to be involved in proteasome-dependent degradation in the cytosol in mammalian cells, the effect of deletion of *PNG1* on the degradation of a mutant carboxypeptidase Y protein, CPY* (Hiller et al., 1996), was examined. CPY* is a well characterized mutant glycoprotein that does not fold correctly and, therefore, is a substrate for proteasomal degradation in yeast. We constructed strains having the *prc1-1* allele, which encodes CPY*, in *png1*Δ and isogenic wild-type strains. The half-life of CPY* was compared in the two strains by pulse–chase experiments. As shown in Fig. 6 (A and B), the *PNG1* gene is not required for CPY* degradation. However, a distinct delay in degradation was seen with the *png1*Δ strain, showing an increase in the half-life of the CPY* protein to 46 min compared with 26 min in the *PNG1* strain. No differences were observed in the vesicular transport of CPY wild-type protein in *png1*Δ and isogenic wild-type strains (data not shown).

In mammalian cells, the involvement of PNGase in pro-

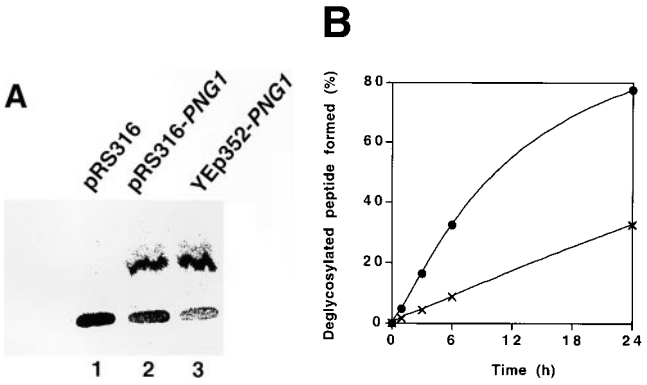

Figure 5. Complementation of the defect of PNGase activity in *png1*Δ cells by plasmids bearing *PNG1*. (A) PNGase activity assay in extract of TSY146 (*png1*Δ) cells with pRS316 (negative control; lane 1), pRS316-*PNG1* (*CEN* plasmid bearing *PNG1*; lane 2) and YEp352-*PNG1* (2-micron plasmid bearing *PNG1*). (B) Time course study of PNGase activity in TSY146 cells bearing pRS316-*PNG1* (*CEN*, x) or YEp352-*PNG1* (2 microns; ●). At the indicated times, an aliquot of reaction mixture was removed and PNGase activity was quantitated using paper chromatography.

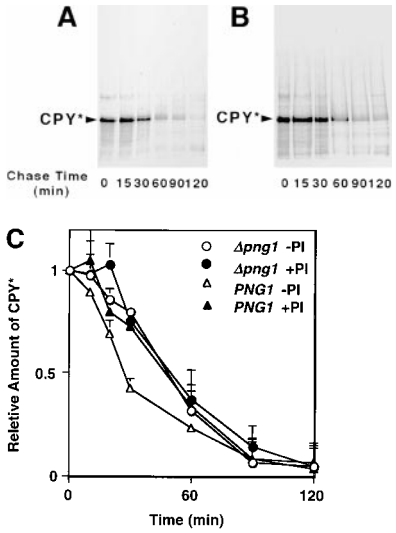

Figure 6. Effect of *png1*Δ on CPY* degradation. Radiolabeled CPY*, prepared as described in Materials and Methods, was analyzed by 7.5% SDS-PAGE, and the labeled protein was visualized using a PhosphorImager. (A) CPY* from TSY147 (BY4742 *prc1-1*); and (B) CPY* from TSY149 (BY4742 *prc1-1 png1*Δ*::KanMX4*). (C) Effect of proteasome inhibitor, MG-132, on the degradation of CPY*. The CPY* recovered by immunoprecipitation at the times indicated was quantitated. PI, proteasome inhibitor (MG-132). The values are the average of three separate experiments and standard errors are indicated. For details, see Materials and Methods.

teasomal degradation was first indicated by the appearance of de-*N*-glycosylated degradation intermediates in the presence of proteasome inhibitors (Wiertz et al., 1996a). In yeast, these inhibitors are ineffective because they cannot enter yeast cells unless the cells have a mutation in the *ERG6* gene, which causes the cells to have increased permeability to a variety of exogenous compounds (Graham et al., 1993). Previously, it has been shown that MG-132, a specific inhibitor of the proteasome, inhibits the degradation of short-lived proteins in an *erg6* mutant background (Lee and Goldberg, 1996). Because the effect of the MG-132 proteasome inhibitor on CPY* degradation had not been examined, we analyzed CPY* destruction in the presence of this inhibitor using the *erg6*Δ strain. As shown in Fig. 6 C, we observed a moderate, but reproducible increase in the half-life for this protein in the presence of the proteasome inhibitor in *PNG1* cells ($t_{1/2}$ = 27 min without MG-132 versus 47 min with MG-132). In sharp contrast to the *PNG1* cells, there was no effect of the proteasome inhibitors on the degradation of CPY* in the *png1*Δ strain ($t_{1/2}$ = 48 min without MG-132 versus 49 min with MG-132; Fig. 6 C). Thus, the lowered rate of degradation of CPY* ($t_{1/2}$ = 46–48 min) was not further decreased by the addition of the proteasome inhibitor. No de-*N*-glycosylated intermediates were observed, even in the presence of MG-132, since there was no change in the position of migration of CPY* with and without the proteasome inhibitor and, in both cases, the CPY* was susceptible to PNGase F digestion (data not shown).

Png1-GFPp Is Found in Both the Nucleus and the Cytosol

Although in earlier studies most of the PNGase activity in a variety of tissues and cells was recovered in the soluble (cytosolic) fraction after subcellular fractionation (Suzuki et al., 1993, 1997, 1998b), the precise subcellular location of the soluble PNGase is still unclear. To localize Png1p in yeast, the green fluorescent protein (GFP) was fused to the COOH terminus of Png1p. Western blotting using anti-GFP mAbs (Fig. 7 A) revealed the absence of immunoreactivity in the *png1*Δ strain (TSY146), whereas a single protein of the expected size (70.5 kD) was detected when TSY146 was transformed with a plasmid containing the *PNG1-GFP* gene. TSY146/pPNG-GFP exhibited PNGase activity, confirming that the Png1-GFPp is enzymatically active (data not shown).

The distribution of Png1-GFPp was analyzed after fixation and staining of the nuclei with DAPI. As seen in Fig. 7 (B and C), the signal was distributed throughout the cells

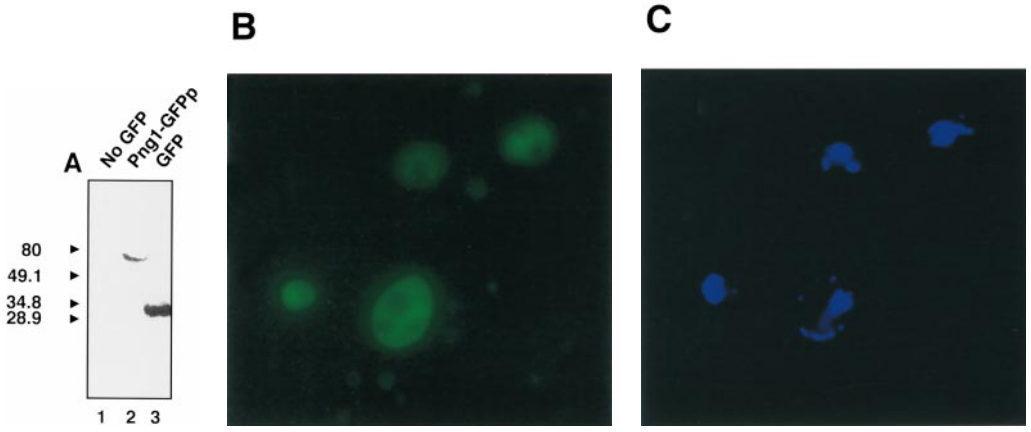

Figure 7. Western blot analysis and subcellular localization of Png1p-GFP fusion protein (Png1-GFPp). (A) Western blotting of Png1-GFPp using anti-GFP antibody. (lane 1) TSY146 cells with pRS316 (*CEN URA3*; Sikorski and Hieter, 1989) as a negative control; (lane 2) TSY146 with pPNG1-GFP (*URA3*); and (lane 3) TSY146 with pGFP-C-FUS (Niedenthal et al., 1996) as a positive control of GFP protein. (B) Localization of Png1-GFPp in *S. cerevisiae*. (C) DAPI staining of the same image shown in B.

with a somewhat stronger signal in the nucleus. Much less staining was observed in large vesicles, which presumably represent vacuoles. These results imply that the protein is localized in the cytosol and nucleus, but is not present in the vesicular compartment.

Sequence Comparison Reveals that the Png1p Is a Highly Conserved Protein in Eukaryotes

To determine the distribution of proteins homologous to yeast Png1p in other eukaryotes, sequence searches were performed using nucleotide/protein databases. By using *S. cerevisiae* Png1p sequence as a query, we found several Png1p homologues ($E < 6e^{-9}$) in various eukaryotes (Table IV). After determining the complete sequence of an IMAGE clone (AI019191), we used it to further carry out EST database surveys and identified several EST clones that consisted of complete or partial ORFs from human (IMAGE clone ID 1316890 from Research Genetics and EST clone accession No. 97076 from ATCC), mouse (IMAGE clone ID 948982), *D. melanogaster* (IMAGE clone ID LD46390), and *C. elegans* (yk491.h3; a gift from Dr. Yuji Kohara). Fig. 8 shows the sequence alignment of *S. cerevisiae* Png1p with *S. pombe*, *C. elegans*, *D. melanogaster*, mouse, and human homologues. The homologues in higher eukaryotes were found to have more extended sequences at both the NH_2 and COOH termini than either *S. cerevisiae* or *S. pombe* Png1p (Fig. 8). However, alignment of the determined sequences revealed a highly conserved core domain present in all eukaryotes examined (Fig. 8). The sequence analysis of *png1-1* allele revealed that the *png1-1* was due to a point mutation of a highly conserved His residue (residue 333 in Fig. 8), which was changed to Tyr, suggesting the importance of this His residue on catalytic activity of Png1p.

Discussion

The functional importance of de-*N*-glycosylation in cellular processes by PNGase was first proposed based on studies in fish oocytes and embryos (Inoue, 1990; Seko et al., 1991). Since then, interest in the biological function of PNGase in somatic eukaryotic cells has grown (Suzuki et al., 1994b, 1995; Berger et al., 1995) and the involvement of mammalian cytosolic PNGases in proteasome-mediated degradation has been proposed (Wiertz et al., 1996a,b). However, because the functional importance of the de-*N*-glycosylation reaction remained unclear in detail, we undertook to study this enzyme in the single cell eukaryote, *S. cerevisiae*. In our initial study (Suzuki et al., 1998b), we demonstrated the presence of PNGase in yeast and showed that it had many of the properties reported for PNGase from higher eukaryotes. In this study, we report the identification of a PNGase activity-defective yeast mutant (*png1-1*) strain. Using this strain, we carried out various genetic approaches that led to the identification of the *PNG1* gene (*YPL096w*). *PNG1* was definitively shown to encode PNGase by carrying out the analysis of reaction product of [^{14}C]asialofetuin glycopeptide I with purified Png1p overexpressed in *E. coli*. Correlation of the expression level of *PNG1* gene and PNGase activity was also confirmed through a complementation experiment using the plasmid borne *PNG1* gene. *PNG1* encodes a soluble protein with no apparent signal sequence. No homologues are present in the *S. cerevisiae* genome, indicating that the gene is not redundant in yeast. This observation is consistent with the finding that deletion of *PNG1* abolishes PNGase activity. Sequence analysis of *png1-1* revealed that the gene encoded a full-length protein corresponding to Png1p with a single mutation of His 218 to Tyr (Fig. 8; residue No. 333), indicating the importance of this His residue in catalytic activity. Indeed, this His residue was found to be conserved for all eukaryotes examined (Fig. 8).

Because the mutant strain did not have a detectable phenotype after several backcrosses to wild-type strains, the isolation of the gene by complementation was problematic. Moreover, the amount of Png1p in yeast cells seems to be very limited; for example, we can detect the PNGase activity only with a highly sensitive method using radioactive glycopeptide as a substrate, and it still requires 12–16 h to detect the activity when the yeast extract is used as an enzyme source (Suzuki et al., 1998b). Indeed, the

*Table IV. S. cerevisiae Png1p-related Sequences Found in Sequence Database**

Accession no.	Definition	E value
AL031852	SPBC1709; *Schizosaccharomyces pombe* chromosome II cosmid c1709	$5e^{-50}$
AI856765	sb41h09.y1 Gm-c1014 *Glycine max* cDNA clone Genome System clone ID: Gm-c1014-282 5′	$1e^{-33}$
AI019191	ub20e10.r1 Soares 2NbMT Mus musculus cDNA clone IMAGE:1378314	$2e^{-29}$
AI491330	486017B11.x2 486 - leaf primordia cDNA library from Hake lab Zea mays cDNA	$5e^{-28}$
AC008339	BACR13P06; *Drosophila melanogaster* chromosome II BAC clone D917	$3e^{-27}$
AL117201	CEY53H1C; *Caenorhabditis elegans* chromosome I cosmid Y53H1C	$6e^{-22}$
Z28729	HSB85D121 Stratagene human skeletal muscle cDNA library, cat. #936215. *Homo sapiens* cDNA clone 85D12	$1e^{-21}$
AI392526	NCSC1A9T3 Subtracted Conidial *Neurospora crassa* cDNA clone SC1A9	$2e^{-16}$
AA139963	mq92e01.r1 Stratagene mouse heart (#937316) *Mus musculus* cDNA clone IMAGE:586200	$7e^{-16}$
AA107311	mp06d11.r1 Life Tech mouse embryo 8 5dpc 10664019 *Mus musculus* cDNA clone IMAGE:568437	$1e^{-12}$
AA786911	m7b03a1.r1 *Aspergillus nidulans* 24 h asexual developmental and vegetative cDNA lambda zap library Emericella nidulans cDNA clone m7b03a1	$2e^{-12}$
AB023033	*Arabidopsis thaliana genomic* DNA, chromosome V, TAC clone: K6M13	$5e^{-9}$
Z81552	*Caenorhabditis elegans* cosmid chromosome I cosmid F56G4	$6e^{-9}$

*Data are from tblastn search using the complete protein sequence of *S. cerevisiae* Png1p as a query. Results are from NCBI database except for AC008339, which was only found from BDGP database.

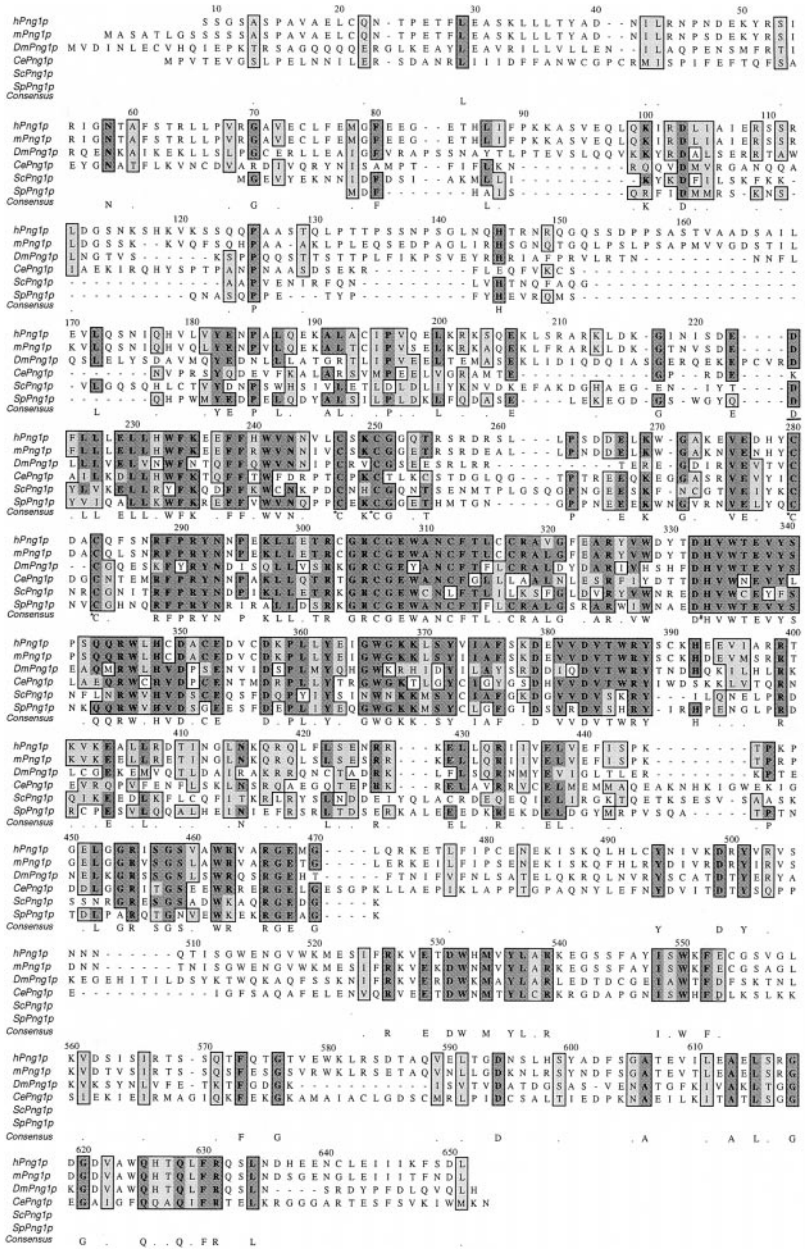

Figure 8. Comparison of sequences of *Png1p* and its homologues. ScPng1p, *S. cerevisiae Png1p*; hPng1p, human Png1p homologue (partial; sequence was determined from EST clone 97076 [ATCC] and IMAGE clone ID 1316890); mPng1p, mouse Png1p homologue (sequence determined from IMAGE clone 948982); DmPng1p, *D. melanogaster* Png1p homologue (sequence determined from IMAGE clone LD46390); CePng1p, *C. elegans* Png1p homologue (sequence determined from yk491h3 and the Entrez database CAB57916); and SpPng1p, *S. pombe* Png1p homologue (sequence obtained from the Entrez database CAA21253). Asterisks represent the conserved cysteine residues in CXYC motifs. The conserved His residue that was found to be mutated to Tyr in the *png1-1* allele is also indicated (#). Numbering is based on the mPng1p sequence.

PNG1 turns out to have significantly low codon usage (codon bias, −0.032), indicating that it would have been extremely difficult to isolate pure Png1p. Therefore, an approach using various genetic methods, as well as application of the yeast genome sequence and the single ORF deletion strains that are commercially available was crucial in identification of the *PNG1* gene.

Whereas the purified enzyme using hexahistidine tag exhibited high PNGase activity toward the glycopeptide substrate (~0.21 μmol/mg protein/min), reactivity toward glycoproteins could not be detected in vitro. This is consistent with the finding that the soluble PNGase, isolated and purified from mammalian cells, also does not act on glycoproteins in vitro (Suzuki et al., 1994a). These observations are reminiscent of the fact that the 20S proteasome can only act primarily on small peptide substrates in vitro, and it has been widely supposed that the function of the 19S ATPases is to unwind protein substrates for them to be substrates for this proteolytic complex (Rubin and Finley, 1995; Wenzel and Baumeister, 1995). The result of the inability of PNGase to act on glycoproteins in vitro may indicate that additional factors are required (as is the case of 20S proteasome) for this enzyme to recognize glycoproteins as substrates in vivo. Currently, we are studying this possibility.

One explanation for the lack of a detectable phenotype in the *png1*Δ strain as well as *png1-1* strain is that the enzyme is not required unless a large amount of misfolded glycoprotein is being produced by the yeast cells. We found that in *png1*Δ cells the rate of degradation of an incorrectly folding mutant protein, CPY* (Hiller et al., 1996) was reduced compared with wild type, suggesting that the gene is at least, to some extent, involved in ER-associated proteasomal degradation. Although our result does not

rule out the possibility that the delay in degradation of CPY* is due to an indirect effect rising from the deletion of Png1p, it is of interest that a number of genes required for this degradation process are nonessential and do not exhibit detectable growth defects under the experimental conditions used (Plemper and Wolf, 1999). These observations imply that the ER quality control machinery seems dispensable under standard laboratory culture conditions, at least in yeast, despite the fact that this process has known to be closely associated with a number of genetic disorders in mammals (Plemper and Wolf, 1999).

When the proteasome inhibitor, MG-132, was added to cells under conditions that are known to inhibit proteasomal degradation (Lee and Goldberg, 1996; Loayza et al., 1998), partial inhibition of degradation of CPY* was observed. This degree of inhibition is consistent with the previous observations on the rate of CPY* degradation using mutated proteasome subunits; with various mutants the $t_{1/2}$ was increased to 2–2.5-fold, but in no case was degradation completely blocked (Hiller et al., 1996). Partial inhibition by the proteasome inhibitor may result because this compound is not effectively taken up by yeast as compared with animal cells (Lee and Goldberg, 1998), or it may be the result of a yet uncharacterized alternative protein degradation system that is not sensitive to this inhibitor. In this connection, it is interesting to note that occurrence of a novel proteolytic complex that can compensate for the essential function of the proteasome recently has been reported in mammalian cells as well as in *S. pombe* (Glas et al., 1998; Geier et al., 1999; Osmulski and Gaczynska, 1999).

We were unable to detect a synergistic effect on CPY* degradation when the proteasome inhibitor was added to the PNGase deletion strain. Unlike mammalian cells, with $PNGase^+$ yeast cells to which proteasome inhibitors had been added, we were unable to detect the accumulation of de-*N*-glycosylated protein intermediates. This finding may mean that de-*N*-glycosylation is a rate-limiting step for proteasome-mediated degradation in yeast, and it may not be possible to detect the de-*N*-glycosylated intermediate under conditions of incomplete inhibition of proteasome activity. In addition, the lack of de-*N*-glycosylated protein intermediates in yeast may indicate that the level of PNGase activity in mammalian cells may be much higher than that in yeast. This hypothesis is consistent with the finding that when small glycopeptides are exported out of the ER to the cytosol, de-*N*-glycosylation occurs immediately in mammalian cells, but not in yeast (Römisch and Ali, 1997; Suzuki et al., 1998b). Since PNGase did not affect glycopeptide export from the ER to the cytosol (Suzuki, T., and W.J. Lennarz, unpublished observations), it is not likely that PNGase is directly involved in the translocation of misfolded proteins from the ER to the cytosol. Rather, it seems that the absence of a PNGase defect somehow slows down proteasomal degradation after the proteins are translocated from the ER to the cytosol or in the case of yeast, to the nucleus.

Although most of the soluble PNGase activity has been described as cytosolic or cytoplasmic, there still is controversy about the precise localization of PNGase in cells (Weng and Spiro, 1997). The primary structure indicates that there is no apparent signal or hydrophobic sequence that could represent a transmembrane domain. This is consistent with the hypothesis that the soluble PNGase does not enter the secretory pathway and, therefore, remains in the cytosol or a topologically equivalent compartment (i.e., the nucleus). Subcellular localization studies of Png1-GFPp in *S. cerevisiae* demonstrated that, although most of the protein is localized in the cytosol, a fraction of the protein is concentrated in the nucleus. At this point, it is not clear if the nucleus-associated protein represents a membrane-associated type of PNGase, which has been described earlier in animal cells (Suzuki et al., 1997; Weng and Spiro, 1997). It is also interesting to note that, unlike multicellular eukaryotes in which proteasomes are abundant in the cytosol, in *S. cerevisiae*, the proteasome is almost exclusively localized in the nucleus (Russell et al., 1999). Since, as discussed above, the soluble PNGase activity may be associated with the proteasomal degradation pathway, the higher concentration of Png1p in the nucleus may indicate colocalization and possible interaction between PNGase and the proteasome machinery in yeast cells.

A careful survey for Png1p homologues in various databases as well as additional sequences of EST clones from various organisms revealed homologues in mammals, plants, insects, nematodes and fungi. These findings demonstrate that this gene is highly conserved evolutionarily throughout eukaryotes. In fact, we have observed PNGase activity when the mouse homologue of Png1p is expressed in *png1*Δ yeast cells, establishing that the mouse homologue is indeed a functional PNGase (Suzuki, T., and W.J. Lennarz, unpublished results). Furthermore, Northern analysis using mouse *PNG1* cDNA as a probe revealed the presence of mRNA in all tissues tested, which is consistent with the biochemical findings of a wide tissue distribution of PNGase activity in mice (Kitajima et al., 1995). Although the functional role of Png1p in cellular processes still remains unclear, the ubiquitous occurrence of this protein in eukaryotes strongly suggests functional significance in certain fundamental biological processes. Finding mutants that are synthetically lethal with *png1*Δ might provide insight into the function of Png1p, and this line of study is currently underway.

As shown in Fig. 8, the *S. cerevisiae* and *S. pombe* PNGases have a core sequence that is highly homologous (amino acid residues 106–362 in ScPng1p) to that found in homologues in higher eukaryotes. In this core, two conserved cysteine residues form CXYC motifs (asterisks). This motif, which is found in the protein disulfide isomerase family, is known to be oxidized to form disulfide bonds. This finding is of interest in view of the fact that reducing reagents such as DTT are required for detection of the PNGase enzyme in in vitro assays (Suzuki et al., 1994a, 1997, 1998b; Kitajima et al., 1995). Perhaps these conserved cysteine residues are important for its catalytic activity. It is also interesting to note that the *C. elegans* homologue has an apparent thioredoxin-like domain in its NH_2 terminus region (66% homologous to the *S. cerevisiae TRX2* gene), and the active site for thioreductase activity (WCGPC) is completely conserved. These findings suggest that the action of PNGase in the cytosol (or nucleus) may somehow be regulated by redox potential. Redox potential is known to be important for ER-associated degra-

dation in mammalian cells (Young et al., 1993; Tortorella et al., 1998), although, thus far, not much is known about its mechanism. Clearly, now that the primary structure of PNGase is known, future studies involving a structure–function approach should answer a number of important questions about the biological importance of this enzyme.

T. Suzuki gratefully acknowledges the continuous encouragement of Drs. Yasuo and Sadako Inoue (Academia Sinica, Taiwan). We also thank Dr. Yasufumi Emori (University of Tokyo) for valuable suggestions on sequence comparison analysis and Dr. Karin Römisch (University of Cambridge) for suggestions on immunoprecipitation. We thank our associates at SUNY at Stony Brook, Drs. Neta Dean, Xiao-Dong Gao, Bernadette Holdener, Janet Leatherwood, Aaron Neiman, Ann Sutton, Dr. Stephan Tafrov, and Mr. David Zappulla for various suggestions and technical comments. We also thank Dr. Shelly Esposito (University of Chicago), Dr. Jacob Winther (Carlberg lab, Copenhagen Valby), Dr. Randy Schekman, Dr. Markus Aebi (ETH, Zürich) and Dr. Yuji Kohara, Dr. JoAnne Engebrecht and Dr. Robert Haltiwanger (SUNY at Stony Brook) for providing various materials. Dr. Jim Trimmer and Mr. Seung-Taek Lim (SUNY at Stony Brook) are thanked for the use of the fluorescent microscope. We gratefully acknowledge members of the Lennarz lab for useful discussions and Ms. Lorraine Conroy for manuscript preparation.

This study was supported by National Institutes of Health grants GM33184 (to W.J. Lennarz), GM50717 (to N.M. Hollingsworth), and GM28220 (to R. Sternglanz). T. Suzuki is a Japan Society for the Promotion of Science (JSPS) Postdoctoral Fellow for Research Abroad.

Submitted: 24 January 2000
Revised: 3 April 2000
Accepted: 6 April 2000

References

Bebök, Z., C. Mazzochi, S.A. King, J.S. Hong, and E.J. Sorscher. 1998. The mechanism underlying cystic fibrosis transmembrane conductance regulator transport from the endoplasmic reticulum to the proteasome includes Sec61β and a cytosolic, deglycosylated intermediary. *J. Biol. Chem.* 273: 29873–29878.

Berger, S., A. Menudier, R. Julien, and Y. Karamanos. 1995. Do de-*N*-glycosylation enzymes have an important role in plant cells? *Biochimie.* 77:751–760.

Brodsky, J.L., and A.A. McCracken. 1999. ER protein quality control and proteasome-mediated protein degradation. *Semin. Cell Dev. Biol.* 10:507–513.

Cresswell, P., and E.A. Hughes. 1997. Protein degradation: the ins and outs of the matter. *Curr. Biol.* 7:R552–R555.

de Virgilio, M., H. Weninger, and N.E. Ivessa. 1998. Ubiquitination is required for the retro-translocation of a short-lived luminal endoplasmic reticulum glycoprotein to the cytosol for degradation by the proteasome. *J. Biol. Chem.* 273:9734–9743.

Elble, R. 1992. A simple and efficient procedure for transformation of yeasts. *Biotechniques.* 13:18–20.

Engebrecht, J., and G.S. Roeder. 1989. Yeast *mer1* mutants display reduced levels of meiotic recombination. *Genetics.* 121:237–247.

Ftouhi-Paquin, N., C.R. Hauer, R.F. Stack, A.L. Tarentino, and T.H. Plummer Jr. 1997. Molecular cloning, primary structure, and properties of a new glycoamidase from the fungus *Aspergillus tubigensis. J. Biol. Chem.* 272:22960–22965.

Geier, E., G. Pfeifer, M. Wilm, M. Lucchiari-Hartz, W. Baumeister, K. Eichmann, and G. Niedermann. 1999. A giant protease with potential to substitute for some functions of the proteasome. *Science.* 283:978–981.

Gillece, P., J.-M. Luz, W.J. Lennarz, F.J. de la Cruz, and K. Römisch. 1999. Export of cysteine-free misfolded secretory protein from the endoplasmic reticulum for degradation required interaction with protein disulfide isomerase. *J. Cell Biol.* 147:1443–1456.

Glas, R., M. Bogyo, J.S. McMaster, M. Gaczynska, and H.L. Ploegh. 1998. A proteolytic system that compensates for loss of proteasome function. *Nature.* 392:618–622.

Graham, T.R., P.A. Scott, and S.D. Emr. 1993. Brefeldin A reversibly blocks early but not late protein transport steps in the secretory pathway. *EMBO (Eur. Mol. Biol. Organ.) J.* 12:869–877.

Halaban, R., E. Cheng, Y. Zhang, G. Moellmann, D. Hanlon, M. Michalak, V. Setaluri, and D.N. Hebert. 1997. Aberrant retention of tyrosinase in the endoplasmic reticulum mediates accelerated degradation of the enzyme and contributes to the dedifferentiated phenotype of amelanotic melanoma cells. *Proc. Natl. Acad. Sci. USA.* 94:6210–6215.

Hammond, C., and A. Helenius. 1995. Quality control in the secretory pathway. *Curr. Opin. Cell Biol.* 7:523–529.

Hartwell, L.H. 1967. Macromolecule synthesis in temperature-sensitive mutants of yeast. *J. Bacteriol.* 93:1662–1670.

Hill, J.E., A.M. Myers, T.J. Koerner, and A. Tzagoloff. 1993. Yeast/*E. coli* shuttle vectors with multiple unique restriction sites. *Yeast.* 2:163–167.

Hiller, M.M., A. Finger, M. Schweiger, and D.H. Wolf. 1996. ER degradation of a misfolded luminal protein by the cytosolic ubiquitin-proteasome pathway. *Science.* 273:1725–1728.

Hollingsworth, N.M., and B. Byers. 1989. *HOP1*: a yeast meiotic pairing gene. *Genetics.* 121:445–462.

Holst, B., A.W. Bruun, M.C. Kielland-Brandt, and J.R. Winther. 1996. Competition between folding and glycosylation in the endoplasmic reticulum. *EMBO (Eur. Mol. Biol. Organ.) J.* 15:3538–3546.

Horton, R.M., Z.L. Cai, S.N. Ho, and L.R. Pease. 1990. Gene splicing by overlap extension: tailor-made genes using the polymerase chain reaction. *Biotechniques.* 8:528–535.

Hughes, E.A., C. Hammond, and P. Cresswell. 1997. Misfolded major histocompatibility complex class I heavy chains are translocated into the cytoplasm and degraded by the proteasome. *Proc. Natl. Acad. Sci. USA.* 94: 1896–1901.

Huppa, J.B., and H.L. Ploegh. 1997. The alpha chain of the T cell antigen receptor is degraded in the cytosol. *Immunity.* 7:113–122.

Inoue, S. 1990. De-*N*-glycosylation of glycoproteins in animal cells. Evidence for occurrence and significance. *Trends Glycosci. Glycotechnol.* 2:225–234.

Jakob, C.A., P. Burda, J. Roth, and M. Aebi. 1998. Degradation of misfolded endoplasmic reticulum glycoproteins in *Saccharomyces cerevisiae* is determined by a specific oligosaccharide structure. *J. Cell Biol.* 142:1223–1233.

Johnston, J.A., C.L. Ward, and R.R. Kopito. 1998. Aggresomes: a cellular response to misfolded proteins. *J. Cell Biol.* 143:1883–1898.

Kitajima, K., T. Suzuki, Z. Kouchi, S. Inoue, and Y. Inoue. 1995. Identification and distribution of peptide:*N*-glycanase (PNGase) in mouse organs. *Arch. Biochem. Biophys.* 319:393–401.

Klapholz, S., and R.E. Esposito. 1982. A new mapping method employing a meiotic Rec⁻ mutant of yeast. *Genetics.* 100:387–412.

Kopito, R.R. 1997. ER quality control: the cytoplasmic connection. *Cell.* 88: 427–430.

Lee, D.H., and A.L. Goldberg. 1996. Selective inhibitors of the proteasome-dependent and vacuolar pathways of protein degradation in *Saccharomyces cerevisiae. J. Biol. Chem.* 271:27280–27284.

Lee, D.H., and A.L. Goldberg. 1998. Proteasome inhibitors: valuable new tools for cell biologists. *Trends Cell Biol.* 8:397–403.

Loayza, D., A. Tam, W.K. Schmidt, and S. Michaelis. 1998. Ste6p mutants defective in exit from the endoplasmic reticulum (ER) reveal aspects of an ER quality control pathway in *Saccharomyces cerevisiae. Mol. Biol. Cell.* 9:2767–2784.

Longtine, M.S., I.A. McKenzie, D.J. Demarini, N.G. Shah, A. Wach, A. Brachat, P. Philippsen, and J.R. Pringle. 1998. Additional modules for versatile and economical PCR-based gene deletion and modification in *Saccharomyces cerevisiae. Yeast.* 14:953–961.

Mosse, C.A., L. Meadows, C.J. Luckey, D.J. Kittlesen, E.L. Huczko, C.L. Slingluff, J. Shabanowitz, D.F. Hunt, and V.H. Engelhard. 1998. The class I antigen-processing pathway for the membrane protein tyrosinase involves translation in the endoplasmic reticulum and processing in the cytosol. *J. Exp. Med.* 187:37–48.

Niedenthal, R.K., L. Riles, M. Johnston, and J.H. Hegemann. 1996. Green fluorescent protein as a marker for gene expression and subcellular localization in budding yeast. *Yeast.* 12:773–786.

Osmulski, P.A., and M. Gaczynska. 1998. A new large proteolytic complex distinct from the proteasome is present in the cytosol of fission yeast. *Curr. Biol.* 8:1023–1026.

Plemper, R.K., and D.H. Wolf. 1999. Retrograde protein translocation: ERADication of secretory proteins in health and disease. *Trends Biochem. Sci.* 24: 266–270.

Römisch, K. 1999. Surfing the Sec61 channel: bidirectional protein translocation across the ER membrane. *J. Cell Sci.* 112:4185–4191.

Römisch, K., and B.R.S. Ali. 1997. Similar processes mediate glycopeptide export from the endoplasmic reticulum in mammalian cells and *Saccharomyces cerevisiae. Proc. Natl. Acad. Sci. USA.* 94:6730–6734.

Rose, M.D., F. Winston, and P. Hieter. 1990. Methods in Yeast Genetics. Cold Spring Harbor Laboratory Press, Cold Spring Harbor, NY. 177 pp.

Rothstein, R. 1991. Targeting, disruption, replacement and allele rescue: integrative transformation in yeast. *Methods Enzymol.* 194:281–301.

Rubin, D.M., and D. Finley. 1995. The proteasome: a protein-degrading organelle? *Curr. Biol.* 5:854–858.

Russell, S.J., K.A. Steger, and S.A. Johnston. 1999. Subcellular localization, stoichiometry, and protein levels of 26 S proteasome subunits in yeast. *J. Biol. Chem.* 274:21943–21952.

Sambrook, J., E.F. Fritsch, and T. Maniatis. 1989. Molecular Cloning. A Laboratory Manual. Second edition. Cold Spring Harbor Laboratory Press, Cold Spring Harbor, NY.

Seko, A., K. Kitajima, Y. Inoue, and S. Inoue. 1991. Peptide:*N*-glycosidase activity found in the early embryos of *Oryzias latipes* (Medaka fish): the first demonstration of occurrence of peptide:*N*-glycosidase in animal cells and its implication for the presence of de-*N*-glycosylation system in living organisms. *J. Biol. Chem.* 266:22110–22114.

Sherman, F. 1991. Getting started with yeast. *Methods Enzymol.* 194:3–21.

Sikorski, R.S., and P. Hieter. 1989. A system of shuttle vectors and yeast host strains designed for efficient manipulation of DNA in *Saccharomyces cerevisiae*. *Genetics.* 122:19–27.

Suzuki, T., and W.J. Lennarz. 2000. In yeast the export of small glycopeptides from the endoplasmic reticulum into the cytosol is not affected by the structure of their oligosaccharide chains. *Glycobiology*. 10:51–58.

Suzuki, T., A. Seko, K. Kitajima, Y. Inoue, and S. Inoue. 1993. Identification of peptide:*N*-glycanase activity in mammalian-derived cultured cells. *Biochem. Biophys. Res. Commun.* 194:1124–1130.

Suzuki, T., A. Seko, K. Kitajima, Y. Inoue, and S. Inoue. 1994a. Purification and enzymatic properties of peptide:*N*-glycanase from C3H mouse-derived L-929 fibroblast cells. Possible widespread occurrence of post-translational remodification of proteins by *N*-deglycosylation. *J. Biol. Chem.* 269:17611–17618.

Suzuki, T., K. Kitajima, S. Inoue, and Y. Inoue. 1994b. Occurrence and biological roles of 'proximal glycanases' in animal cells. *Glycobiology*. 4:777–789.

Suzuki, T., K. Kitajima, S. Inoue, and Y. Inoue. 1995. *N*-glycosylation/deglycosylation as a mechanism for the post-translational modification/remodification of proteins. *Glyco. J.* 12:183–193.

Suzuki, T., K. Kitajima, Y. Emori, Y. Inoue, and S. Inoue. 1997. Site-specific de-*N*-glycosylation of diglycosylated ovalbumin in hen oviduct by endogenous peptide:*N*-glycanase as a quality control system for newly synthesized proteins. *Proc. Natl. Acad. Sci. USA*. 94:6244–6249.

Suzuki, T., Q. Yan, and W.J. Lennarz. 1998a. Complex, two-way traffic of molecules across the membrane of the endoplasmic reticulum. *J. Biol. Chem*. 273: 10083–10086.

Suzuki, T., H. Park, K. Kitajima, and W.J. Lennarz. 1998b. Peptides glycosylated in the endoplasmic reticulum of yeast are subsequently deglycosylated by a soluble peptide:*N*-glycanase activity. *J. Biol. Chem*. 273:21526–21530.

Tarentino, A.L., G. Quinones, A. Trumble, L.M. Changchien, B. Duceman, F. Maley, and T.H. Plummer Jr. 1990. Molecular cloning and amino acid sequence of peptide-N^4-(*N*-acetyl-beta-D-glucosaminyl)asparagine amidase from *Flavobacterium meningosepticum*. *J. Biol. Chem*. 265:6961–6966.

Tortorella, D., C.M. Story, J.B. Huppa, E.J. Wiertz, T.R. Jones, and H.L. Ploegh. 1998. Dislocation of type I membrane proteins from the ER to the cytosol is sensitive to changes in redox potential. *J. Cell Biol.* 142:365–376.

Weng, S., and R.G. Spiro. 1997. Demonstration of a peptide:*N*-glycosidase in the endoplasmic reticulum of rat liver. *Biochem. J.* 322:655–661.

Wenzel, T., and W. Baumeister. 1995. Conformational constraints in protein degradation by the 20S proteasome. *Nat. Struct. Biol.* 2:199–204.

Wiertz, E.J., T.R. Jones, L. Sun, M. Bogyo, H.J. Geuze, and H.L. Ploegh. 1996a. The human cytomegalovirus US11 gene product dislocates MHC class I heavy chains from the endoplasmic reticulum to the cytosol. *Cell.* 84:769–779.

Wiertz, E.J., D. Tortorella, M. Bogyo, J. Yu, W. Mothes, T.R. Jones, T.A. Rapoport, and H.L. Ploegh. 1996b. Sec61-mediated transfer of a membrane protein from the endoplasmic reticulum to the proteasome for destruction. *Nature.* 384:432–438.

Yan, Q., G.D. Prestwich, and W.J. Lennarz. 1999. The Ost1p subunit of yeast oligosaccharyl transferase recognizes the peptide glycosylation site sequence, -Asn-X-Ser/Thr-. *J. Biol. Chem*. 274:5021–5025.

Yang, M., S. Omura, J.S. Bonifacino, and A.M. Weissman. 1998. Novel aspects of degradation of T cell receptor subunits from the endoplasmic reticulum (ER) in T cells: importance of oligosaccharide processing, ubiquitination, and proteasome-dependent removal from ER membranes. *J. Exp. Med.* 187: 835–846.

Young, J., P.L. Kane, M. Exley, and T. Wileman. 1993. Regulation of selective protein degradation in the endoplasmic reticulum by redox potential. *J. Biol. Chem*. 268:19810–19818.

Yu, H., G. Kaung, S. Kobayashi, and R.R. Kopito. 1997. Cytosolic degradation of T-cell receptor alpha chains by the proteasome. *J. Biol. Chem*. 272:20800–20804.